Disturbance Rejection Properties for a 5G Networked Data Flow Delay Controller

Katrina Lau, Torbjörn Wigren, Ramón Delgado and Richard H. Middleton

***Abstract*— Radio transmission at millimeter wave carrier frequencies will be a central technology in the new 5G wireless systems that are in standardization. To obtain a sufficient coverage, multi-point transmission is needed to compensate for the severe radio shadowing that occurs at these frequencies. Incoming downlink data streams must then be split and sent on to the radio base stations over multiple data paths, often with different delay properties. This paper presents a new MIMO delay skew control algorithm that operates over these paths to secure simultaneous transmission over the corresponding wireless interfaces. This secures redundancy gains for ultra-reliable communication applications. The paper also presents an analysis of disturbance rejection and reference signal tracking properties, arriving at conditions that decouple these properties between the control channels. These conditions provide guidelines for network design.**

I. Introduction

Networked control systems (NCSs) operating over combined internet and wireless interfaces typically assume that sampling rates and delays over the control and feedback signal paths are kept constant and within specified ranges. In case of violation, NCS application deployments would become complicated with significant performance and stability issues [1]. Currently new fifth generation (5G) wireless standards operating at millimeter wave frequency bands are in standardization, see e.g. [2], [3], [4]. At these frequency bands extensive radio shadowing reduces the coverage, something that needs to be counteracted with so called multi-point transmission [2], [4], [5]. Multi-point transmission means that incoming data streams are split at a network node closer to the data source than the transmission nodes, i.e. the radio base stations. Since the fronthaul connections between the node that performs the data split and the transmission nodes may be implemented with different technologies, including optical fibre, copper wire and radio, the delay characteristics may also be different between the data paths. Another reason for this delay variation is that the fronthaul data paths are shared between thousands of users and sometimes between different radio access networks (RANs). The corresponding load variations can then generate delay differences. In addition to considering the effects of delays, the literature on networked control system has analyzed effects of quantization [6], [7], [8]. However, this is not within the scope of this paper.

Katrina Lau, Ramon Delgado and Richard H. Middleton are with the Priority Research Centre for Complex Dynamic Systems and Control, The University of Newcastle, Callaghan, NSW 2308, AUSTRALIA. e-mail: {k.lau, ramon.delgado, richard.middleton }@newcastle.edu.au.

Torbjörn Wigren is with L5GR Systems, Ericsson AB, Stockholm, SE-16480 Sweden. e-mail: torbjorn.wigren@ericsson.com.

In response to the expected impacts of wireless delay on control system performance associated with the new 5G machine type communication (MTC) use cases, a call for a renewed study of delays in networked control was issued in [9]. The present paper therefore contributes with a new multiple-input-multiple-output (MIMO) controller that operates below the 5G application layer.

The proposed algorithm controls the delay skews between the $n+1$ data paths, as counted from the controlling node where the data split occurs, over the fronthaul interfaces, to the wireless interface at the transmission node. The selected control objective is suitable to secure simultaneous transmission in the downlink, something that is needed to secure the combining gains needed for example for ultra-reliable MTC. The data buffers at the transmission nodes are used as actuators to vary the downlink delays. By varying the incoming data rates to these buffer, the data volumes are varied, which translates to a variation of the dwell times of each piece of data in the buffers. The controller employs cascade control, using the single-input-single-output (SISO) inner loop controllers described in [10] to control the data rates of the transmission over the fronthaul interfaces. It is stressed that this approach automatically solves the general $n+1$-node nonlinear data split control problem since the data rates over the fronthaul interfaces fully define the data split as a momentary data rate command budget, for each data path.

The second contribution of the paper is the analysis of the performance of the MIMO controller and quantification of reference signal tracking and disturbance rejection performance properties for the $n+1$-node case. It is found that a symmetric design of the data paths has distinct advantages, among these reference signal tracking decoupling. In addition, if the inner loops tend to perfection as seen from the outer MIMO loop, then disturbance rejection for the delay skews follows. These results provide key guidelines for the design of delay critical 5G networks. It is noted that [11] provides similar results for the two node case.

Previous work on flow control over combined internet and wireless interfaces includes the internet transmission control protocol (TCP) algorithms [12]. These algorithms are very often enhanced with active queue management (AQM) algorithms that improve performance by intentionally discarding data packets when buffers grow too much [12]. In 5G, data streams may also need to be split to meet other control objectives than the downlink wireless transmission alignment studied in the present paper, [13], [14] and [11]. The papers [1] and [15] discuss *round trip delay*

Peer-reviewed author's copy of:
K. Lau, T. Wigren, R. Delgado and R. H. Middleton. **Disturbance rejection properties for a 5G networked data flow delay controller**. In *IEEE 56th Annual Conference on Decision and Control (CDC)*, Melbourne, Australia, 2017.
Available at https://doi.org/10.1109/CDC.2017.8263892

skew controllers suitable for so called critical machine type communications (C-MTC) where the *control loop delays* of feedback control applications need to be guaranteed. Such a change of control objective may seem subtle, but it leads to significant algorithmic modifications including different external signals and inner loop controllers [16]. The stability of the $n+1$-node downlink delay skew control algorithm proposed here is analyzed with integral quadratic constraint (IQC) theory ([17]) in [13], [14]. The two node downlink control case was treated by a combination of the classical single input single output (SISO) Nyquist and Popov criteria in [11]. A similar approach was used to analyze the stability of the two node round trip delay skew controller in [1]. The stability of the $n+1$-node round trip delay control case was established in [15] using IQC theory. Finally it is noted that the present paper assumes linearity, while the stability analysis of [13], [14] utilizes the full non-linear networked system model with multiple inner-loop data rate saturations.

The paper is organized as follows. Section II presents the networked control system. This is followed by an analysis of the tracking and disturbance rejection performance in Section III. The controller performance is illustrated numerically in Section IV, where results from a testbed are presented. Concluding remarks close the paper in Section V.

II. Downlink Delay Skew Control

A. Overview

The block diagram of the MIMO downlink delay skew controller appears in Fig. 1. As can be seen, cascade control is applied. There is an outer delay skew control loop with $n+1$ reference signal inputs and $n+1$ delay skew and delay sum outputs. The controller exploits static decoupling, which allows each control channel filter to be individually designed without consideration of cross coupling. Each outer loop control channel provides queue dwell time reference values to the inner SISO control loops. The inner loops perform the downlink delay control, by variation of the data volume of the transmit data queue of each transmission node.

The present paper is based on a linear analysis of the system shown in Fig. 1. It is noted that this assumes that saturations (positivity constraints) on the inner loop queue dwell time reference values are not active. This is a valid assumption whenever the signal $T_{sum}^{ref}(s)$ is selected large enough. The consequence is that the reference queue dwell time signals are also large. Therefore also the inner loops operate without nonlinear effects that would otherwise be caused by a need to restrict the commanded data flow rate to positive values.

The following assumption on stability is assumed to hold for the linear delay skew control system of Fig. 1.

A1) The NCS of Fig. 1 is stable without poles on the imaginary axis (IQC guarantees stability in the $\mathcal{L}_2$ sense).

See [17] for details of the IQC stability concept. Conditions that imply A1 are derived in [13], [14].

B. The Outer Loop

The outer loop feedback controller is assumed to be located in the node where the split of the data stream takes place. The control loop is composed of n delay skew control channels and one delay sum control channel. The objective of the delay skew control channels is to regulate the measured output signals $T_{skew,i}(s)$, $i=1,...,n$, so that the reference downlink delay skews $T_{skew,i}^{ref}(s)$, $i=1,...,n$, are well tracked. The reference value $T_{sum}^{ref}(s)$ of the delay sum channel sets the total available delay that is to be distributed between the data paths to meet each $T_{skew,i}^{ref}(s)$, $i=1,...,n$. In order to be able to meet the delay skew reference values, $T_{sum}^{ref}(s)$ needs to be large enough to provide positive queue dwell time reference values $T_i^{ref}(s)$, $i=1,...,n,r$ to the corresponding inner loops. Here the subscript r denotes the reference data path corresponding to the delay sum control channel. Further details on how to set a consistent value of $T_{sum}^{ref}(s)$ appears in example 1 of [15].

The outer loop computes the control errors $e_i(s)$, $i=1,...,n,r$, and the corresponding control signals $u_i(s)$, $i=1,...,n,r$, as follows

$$e_i(s) = T_{skew,i}^{ref}(s) - T_{skew,i}(s), \quad i=1,...,n, \tag{1}$$

$$e_r(s) = T_{sum}^{ref}(s) - T_{sum}(s), \tag{2}$$

$$u_i(s) = C_{skew,i}(s)e_i(s), \quad i=1,...,n, \tag{3}$$

$$u_r(s) = C_{sum}(s)e_r(s). \tag{4}$$

The controller filters $C_{skew,i}(s)$, $i=1,...,n$, and $C_{sum}(s)$ can be designed with any suitable method for SISO linear controller design. However, as has been proved in [18], it is essential not to use a low frequency gain that is too large, since that may compromise stability for large delays. In Section IV and in [13], classical lead-lag links are used, cf. [10] and [11].

The control signals are then fed into the static decoupling network, defined by the decoupling matrix $\mathbf{M}$. Theorem 1 of [15] shows that the decoupling matrix can be analytically computed as

$$\mathbf{M} = \frac{1}{n+1}\begin{pmatrix} n & -1 & \cdots & \cdots & -1 & 1 \\ -1 & n & -1 & \cdots & -1 & 1 \\ \vdots & \ddots & \ddots & \ddots & -1 & 1 \\ \vdots & \vdots & \ddots & \ddots & -1 & 1 \\ -1 & \cdots & \cdots & -1 & n & 1 \\ -1 & \cdots & \cdots & \cdots & -1 & 1 \end{pmatrix}. \tag{5}$$

The proof is straightforward and obtained by considering the steady state version of Fig. 1. It follows that the outputs of the decoupling matrix are given by

$$T_i^{ref}(s) + T_i^{DL}(s)$$

$$= \sum_{k=1}^{n} m_{i,k}u_k(s) + m_{i,n+1}u_r(s), \quad i=1,...,n, \tag{6}$$

$$T_r^{ref}(s) + T_r^{DL}(s)$$

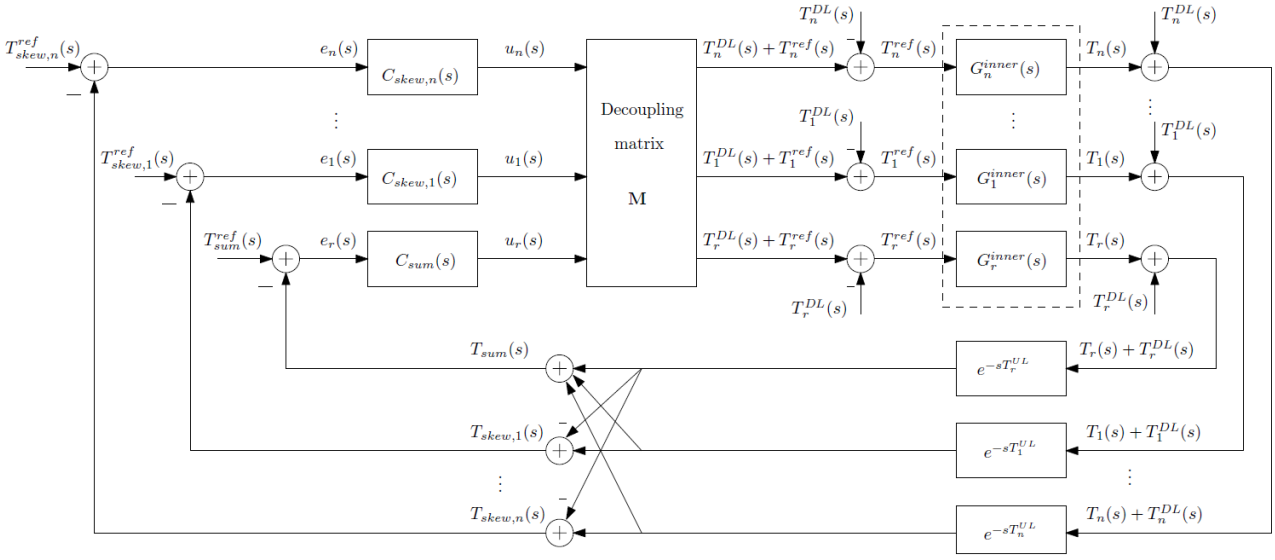

Fig. 1. Block diagram of the networked $n+1$-node downlink delay skew control system.

$$= \sum_{k=1}^{n} m_{n+1,k} u_k(s) + m_{n+1,n+1} u_r(s), \tag{7}$$

where $m_{i,j}$, $i = 1, ..., n+1$, $j = 1, ..., n+1$ are the elements of $\mathbf{M}$. Note that the subscripts $_r$ and $_{n+1}$ coincide.

Since the objective is to control the queue dwell times of the transmission nodes, the downlink fronthaul delays $T_i^{DL}(s)$, $i = 1, ..., n, r$, of each connection between the data split node and a transmission node needs to be measured and subtracted from $T_i^{ref}(s) + T_i^{DL}(s)$, $i = 1, ..., n, r$. As seen in Fig. 1, the inner loops are modeled by the linear transfer functions $G_i^{inner}(s)$ discussed in Section II-C. The resulting queue dwell times $T_i(s)$, $i = 1, ..., n, r$, hence become

$$T_i(s) = G_i^{inner}(s) T_i^{ref}(s), \quad i = 1, ..., n, r. \tag{8}$$

Noting that the control objective is to control the delay differences between the different data paths, as counted from the data splitting node to the wireless interfaces of each transmission node, it follows that the signals $T_i(s) + T_i^{DL}(s)$, $i = 1, ..., n, r$, need to be formed. These signals are sent from the transmission nodes to the data split node, thereby experiencing an uplink delay T_i^{UL}, $i = 1, ..., n, r$. This delay is subject to the following assumption:

A2) The uplink delays T_i^{UL}, $i = 1, ..., n, r$ are constant.

This allows the delay sum and delay skew output signals to be formed in the outer loop controller as

$$T_{skew,i}(s) = e^{-sT_i^{UL}} (T_i(s) + T_i^{DL}(s)) - e^{-sT_r^{UL}} (T_r(s) + T_r^{DL}(s)), \quad i = 1, ..., n, \tag{9}$$

$$T_{sum}(s) = \sum_{i=1}^{n} e^{-sT_i^{UL}} (T_i(s) + T_i^{DL}(s)) + e^{-sT_r^{UL}} (T_r(s) + T_r^{DL}(s)). \tag{10}$$

Note that the uplink delays are treated as fixed as seen by the outer loop, while the downlink delays are treated as dynamic signals.

C. The Inner Loops

The delay skew controller studied in this paper and [13] utilises inner loops of the form described in [10]. A block diagram of one of the inner loops is depicted in Fig. 2. Methods for designing the inner loop controllers are discussed in both [10] and [18]. Each inner loop first transforms the reference queue dwell time value $T_i^{ref}(t)$, $i = 1, ..., n, r$ to a corresponding queue data volume reference $y_i^{ref}(t)$, $i = 1, ..., n, r$, by a multiplication with the momentary wireless data rate, $w_{air,i}(t)$. As explained in [10], this embeds time invariant inner feedback loops with the queue data volumes $y_i(t)$, $i = 1, ..., n, r$, as the output signals. The queue dwell times are then obtained by divisions with the wireless data rate of each transmission node. As expressed by the Laplace variable s appearing in $y_i(s)$ of Fig. 2, the inner time invariant loops can be described equally well in the frequency domain. The inner feedback loops are hence closed from the queue data volumes rather than from the queue dwell times, to enable time invariant design. To describe the inner loops further, the feedback controller filters $C_i(s)$, $i = 1, ..., n, r$ are selected as lead-lag filters

$$C_i(s) = K \frac{s+a}{s+\frac{a}{M}} N \frac{s+b}{s+Nb}, \quad i = 1, ..., n, r. \tag{11}$$

Each inner loop is also subject to rate saturation, reflecting the fact that the data rates are non-negative. These saturations are assumed to be inactive in the present paper, but retained in the stability analysis of [13]. After the fronthaul transmission delay the control signal affects the queue data volume dynamics, $G_{queue,i}(s)$, $i = 1, ..., n, r$, of each inner

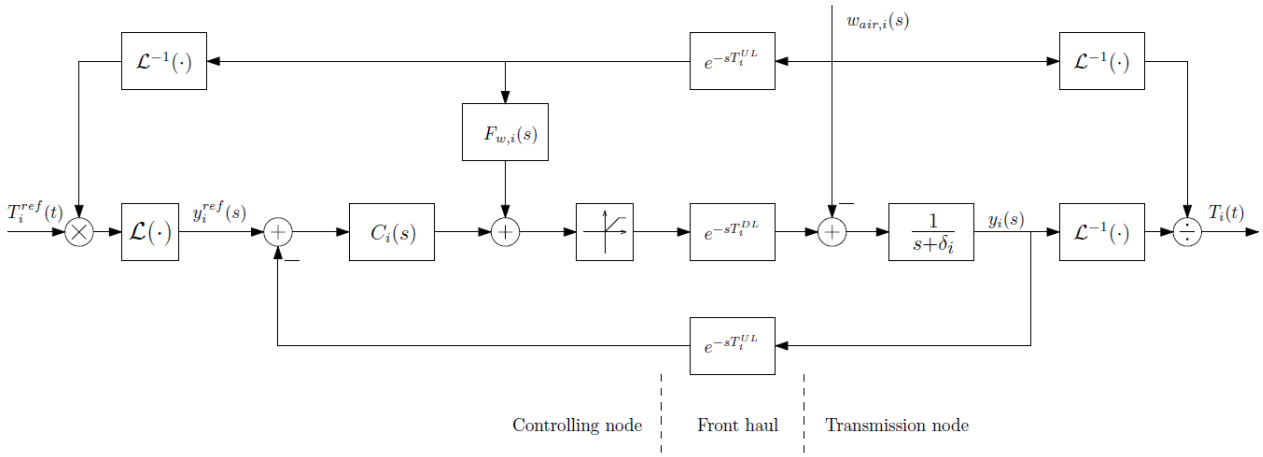

Fig. 2. Block diagram of one of the inner loops that controls the queue data volume and, indirectly, the queue dwell time. In the figure $\mathcal{L}(\cdot)$ denotes Laplace transformation.

loop in the following way

$$y_i(s) = G_{queue,i}(s)\left(u_{inner,i}(s) - w_{air,i}(s)\right)$$
$$= \frac{1}{s+\delta_i}\left(u_{inner,i}(s) - w_{air,i}(s)\right), \quad i = 1, ..., n, r, \quad (12)$$

where $u_{inner,i}(s)$, $i = 1, ..., n, r$ denote the control signals after the fronthaul connections and where $w_{air,i}(s)$, $i = 1, ..., n, r$ denote the air interface data rates that empty the queues. The queues are modeled by leaky integrators, where the parameters δ_i, $i = 1, ..., n, r$, represent leakage caused by AQM packet discards [10]. The inner loop controllers may also employ optional feedforward, to improve the attenuation of the air-interface data rate disturbances. Standard second order feedforward controller filters given by

$$F_{w,i}(s) = \frac{\omega_{0,i}^2}{s^2 + 2\xi_{0,i}\omega_{0,i}s + \omega_{0,i}^2}, \quad i = 1, ..., n, r \quad (13)$$

are then used. Here $\omega_{0,i}$ are the bandwidths and $\xi_{0,i}$ the damping parameters. In the analysis of the present paper, feedforward effects are however not included. Finally, the fronthaul affects the control loop with both downlink and uplink delays, modeled as $e^{-sT_i^{DL}}$, $i = 1, ..., n, r$ and $e^{-sT_i^{UL}}$, $i = 1, ..., n, r$, respectively.

Since cascade control is applied, the reference values $T_i^{ref}(s)$, $i = 1, ..., n, r$, provided by the outer loop have significantly lower bandwidths than the inner loops themselves. This fact allows the embedding to be neglected for the outer loop, as manifested by (8). This can be seen by noting that the following relation holds

$$T_i(t) = \frac{1}{w_{air,i}(t)}\mathcal{L}^{-1}(y_i(s))$$
$$= \frac{1}{w_{air,i}(t)}\mathcal{L}^{-1}\left(G_i^{inner}(s)\mathcal{L}\left((T_i^{ref}(t)w_{air,i}(t)\right)\right). \quad (14)$$

The time scales of the fast variations of $w_{air,i}(t)$ and the slow variations of the reference delays from the outer loop can now be separated. To do so averaging over the fast variations is applied, while the remaining variables are treated as constants. This gives

$$T_i(t)$$
$$= \frac{1}{\bar{w}_{air,i}}\mathcal{L}^{-1}\left(G_i^{inner}(s)T_i^{ref}(s)\right)\bar{w}_{air,i}, \quad i = 1, ..., n, r, \quad (15)$$

where $\bar{w}_{air,i}$, $i = 1, ..., n, r$, are the average scheduled bit rates. The above argument is formalized by the following assumptions:

A3) The bandwidths of $w_{air,i}(t)$, $i = 1, ..., n, r$, are significantly higher than the bandwidths of the reference values produced by the outer delay skew loop. The following relations therefore hold
   a) $(w_{air,i}(t))^{-1} \approx (\bar{w}_{air,i})^{-1}$, $i = 1, ..., n, r$.
   b) $\mathcal{L}\left(T_i^{ref}(t)w_{air,i}(t)\right) \approx T_i^{ref}(s)\bar{w}_{air,i}$, $i = 1, ..., n, r$.

A4) The inner loops operate as intended, with the data flow rate saturation inactive.

Using A3 and A4 to evaluate (9) and (10), the effect of $w_{air,i}(t)$, $i = 1, ..., n, r$, at the input and the output of the inner loops cancel and (8) holds.

The transfer functions of the inner loops can now be computed. In order to do this, the inner loops are first represented by loop gains, $\hat{g}_i(s)$, $i = 1, ..., n, r$, where it is assumed that A4 holds. Note that the loop gains are defined without delays, with the delays being added separately. The loop gains take the form

$$\hat{g}_i(s) = C_i(s)G_{queue,i}(s), \quad i = 1, ..., n, r. \quad (16)$$

Each $G_{queue,i}(s)$ is hence typically given by an integrator or, with AQM, a leaky integrator. The inner loop transfer functions are then given by

$$G_i^{inner}(s) = \frac{G_{0,i}\hat{g}_i(s)e^{-sT_i^{DL}}}{1 + \hat{g}_i(s)e^{-s(T_i^{DL}+T_i^{UL})}}, \quad i = 1, ..., n, r, \quad (17)$$

where $G_{0,i},\ i = 1, ..., n, r$ represent reference signal gains, which are used to adjust the static gains. It is stressed again that the inner loop feedforward controller paths are not included in the present analysis.

Note that T_i^{DL}, $i = 1, ..., n, r$, denotes the average downlink delay of each inner loop. This means that the modeling of the inner and outer loops differ. The inner loops are modeled with nominal average delays, while the outer loop treats the downlink delays as external signals. This difference represents an approximation motivated by the approach to analyze the networked control loop with linear time invariant methods. The following assumption is therefore used in the paper:

A5) The inner loops can be characterized by the average downlink delays T_i^{DL}, $i = 1, ..., n, r$, where $T_i^{DL}(t) = T_i^{DL} + \Delta T_i^{DL}(t)$, $i = 1, ..., n, r$.

III. Reference Tracking and Disturbance Rejection

A. A MIMO State Space Model

In order to define a state space model for the downlink delay skew control system it is first assumed that

A6) The reference values $T_i^{ref}(t) \geq 0.0$, $i = 1, ..., n, r$.

With this assumption, the saturation on the inner loop queue dwell time references can be omitted, and a linear analysis can be performed. By following the outer control loop of Fig. 1 from the outputs to the control errors, it follows that

$$\begin{pmatrix} T_{skew,1}(s) \\ \vdots \\ T_{skew,n}(s) \\ T_{sum}(s) \end{pmatrix} = \mathbf{A}(s) \begin{pmatrix} e_1(s) \\ \vdots \\ e_n(s) \\ e_r(s) \end{pmatrix} + \mathbf{B}(s) \begin{pmatrix} T_1^{DL}(s) \\ \vdots \\ T_n^{DL}(s) \\ T_r^{DL}(s) \end{pmatrix}. \quad (18)$$

An introduction of the control error formation and a rearrangement then results in

$$\begin{pmatrix} T_{skew,1}(s) \\ \vdots \\ T_{skew,n}(s) \\ T_{sum}(s) \end{pmatrix} = (\mathbf{I} + \mathbf{A}(s))^{-1} \mathbf{A}(s) \begin{pmatrix} T_{skew,1}^{ref}(s) \\ \vdots \\ T_{skew,n}^{ref}(s) \\ T_{sum}^{ref}(s) \end{pmatrix} + (\mathbf{I} + \mathbf{A}(s))^{-1} \mathbf{B}(s) \begin{pmatrix} T_1^{DL}(s) \\ \vdots \\ T_n^{DL}(s) \\ T_r^{DL}(s) \end{pmatrix}. \quad (19)$$

This equation is a vector equivalent to the classical reference tracking and disturbance rejection tradeoff equation, with the last term being related to the sensitivity function, c.f. [19]. The downlink delay vector represents the disturbance.

The elements of the matrices $\mathbf{A}(s)$ and $\mathbf{B}(s)$ follow from Fig. 1 and (1)–(10). Due to space limitations the end result is not reproduced here, instead two special cases are treated below. To motivate these, note that the static reference signal tracking properties are good when $\|\mathbf{A}(0)\|$ is large. Since it turns out that $\mathbf{B}(s)$ is neither dependent on $C_{skew,i}(s)$, $i = 1, ..., n$, nor on $C_{sum}(s)$, it follows that a large $\|\mathbf{A}(0)\|$ also gives good disturbance rejection properties. There is however an inherent stability problem. As shown in [18] large loop delays tend to destabilize loops like the one above, unless the low frequency gain is limited.

It is therefore relevant to ask if there are other ways to achieve reference tracking and disturbance rejection?

B. Decoupled Reference Tracking

In order to study the reference tracking performance, the following assumptions are introduced

A7) $\hat{g}_1(s) = \hat{g}_2(s) = ... = \hat{g}_n(s) = \hat{g}_r(s)$.

A8) $|T_i^{UL} - T_j^{UL}| \leq \varepsilon,\ i = 1, ..., n, r,\ j = 1, ..., n, r$, for some $\varepsilon \geq 0$.

Straightforward computations using the components of $\mathbf{A}(s)$ then reveal that $\mathbf{A}(s)$ is asymptotically diagonal (as $\varepsilon \to 0$) with elements given by

$$A_{(i)(i)}(s) = C_{skew,i}(s) G_i^{inner}(s) e^{-sT_i^{UL}} + C_i\varepsilon,\ i = 1, ..., n, \quad (20)$$

$$A_{(n+1)(n+1)}(s) = C_{sum}(s) G_r^{inner}(s) e^{-sT_r^{UL}} + C_{n+1}\varepsilon, \quad (21)$$

and with the non-diagonal elements satisfying

$$|A_{(i)(j)}(j\omega)| \leq C_{i,j}\varepsilon,\ i, j = 1, ..., n+1, i \neq j, \quad (22)$$

$\forall\omega$, where C_i and $C_{i,j}$ denote positive constants. This is exactly what the static decoupling (5) was designed to give. A further evaluation of the components of (19) results in the following result:

Theorem 1: Assume that A1–A8 hold with $\varepsilon = 0$. Then

$$T_{skew,i}(s) = \frac{C_{skew,i}(s) G_i^{inner}(s) e^{-sT_i^{UL}}}{1 + C_{skew,i}(s) G_i^{inner}(s) e^{-sT_i^{UL}}} T_{skew,i}^{ref}(s) + \frac{\left(1 - G_i^{inner}(s)\right) e^{-sT_i^{UL}}}{1 + C_{skew,i}(s) G_i^{inner}(s) e^{-sT_i^{UL}}} T_i^{DL}(s) - \frac{\left(1 - G_r^{inner}(s)\right) e^{-sT_r^{UL}}}{1 + C_{skew,i}(s) G_i^{inner}(s) e^{-sT_i^{UL}}} T_r^{DL}(s),\ i = 1, ..., n,$$

$$T_{sum}(s) = \frac{C_{sum}(s) G_r^{inner}(s) e^{-sT_r^{UL}}}{1 + C_{sum}(s) G_r^{inner}(s) e^{-sT_r^{UL}}} T_{sum}^{ref}(s) + \frac{\left(1 - G_r^{inner}(s)\right) e^{-sT_r^{UL}}}{1 + C_{sum}(s) G_r^{inner}(s) e^{-sT_r^{UL}}} T_r^{DL}(s) + \sum_{i=1}^{n} \frac{\left(1 - G_i^{inner}(s)\right) e^{-sT_i^{UL}}}{1 + C_{sum}(s) G_r^{inner}(s) e^{-sT_r^{UL}}} T_i^{DL}(s).$$

The conclusion is that good reference tracking properties follow when the delay skew controller possesses symmetry between the data paths.

C. Disturbance Rejection

In order to also secure disturbance rejection, the following additional assumption is needed

A9) $|G_i^{inner}(j\omega) - 1| \leq \delta$, $\delta > 0$, $i = 1, ..., n, r$, when $\omega \leq \omega_{outer}$, where ω_{outer} denotes the outer delay skew control loop bandwidth.

Using this assumption, together with A7, A8 and $\varepsilon = 0$ first allows the two disturbance terms of $T_{skew,i}(s)$ of Theorem 1 to be estimated as follows, assuming that $\omega \leq \omega_{outer}$

$$\left| \frac{\left(1 - G_i^{inner}(j\omega)\right) e^{-j\omega T_i^{UL}}}{1 + C_{skew,i}(j\omega) G_i^{inner}(j\omega) e^{-j\omega T_i^{UL}}} T_i^{DL}(j\omega) \right.$$

$$\left. - \frac{\left(1 - G_r^{inner}(j\omega)\right) e^{-j\omega T_r^{UL}}}{1 + C_{skew,i}(j\omega) G_i^{inner}(j\omega) e^{-j\omega T_i^{UL}}} T_r^{DL}(j\omega) \right|$$

$$= \left| \frac{\left(1 - G_i^{inner}(j\omega)\right) e^{-j\omega T_i^{UL}}}{1 + C_{skew,i}(j\omega) G_i^{inner}(j\omega) e^{-j\omega T_i^{UL}}} \right|$$

$$\times |T_i^{DL}(j\omega) - T_r^{DL}(j\omega)|$$

$$\leq \delta K_i |T_i^{DL}(j\omega) - T_r^{DL}(j\omega)|, \quad i = 1, ..., n. \tag{23}$$

Here K_i is a constant formed from the components of the denominators of the transfer functions. K_i is bounded because of A1. The results are summarized in:

Theorem 2: Assume that A1–A9 hold with $\varepsilon = 0$. Then there are constants $K_i < \infty$, $i = 1, ..., n$, such that for $\omega \leq \omega_{outer}$,

$$\left| \frac{\left(1 - G_i^{inner}(j\omega)\right) e^{-j\omega T_i^{UL}}}{1 + C_{skew,i}(j\omega) G_i^{inner}(j\omega) e^{-j\omega T_i^{UL}}} T_i^{DL}(j\omega) \right.$$

$$\left. - \frac{\left(1 - G_r^{inner}(j\omega)\right) e^{-j\omega T_r^{UL}}}{1 + C_{skew,i}(j\omega) G_i^{inner}(j\omega) e^{-j\omega T_i^{UL}}} T_r^{DL}(j\omega) \right|$$

$$\leq \delta K_i |T_i^{DL}(j\omega) - T_r^{DL}(j\omega)|, \quad i = 1, ..., n.$$

It can be concluded that good delay skew disturbance rejection properties follow when the inner loops are well defined, in addition to the symmetry required for reference signal tracking.

IV. Numerical Results

The C++ testbed code described in [11] and [15] was used to setup a scenario with 5 data paths. Different realizations of a 3 $kmph$ typical urban channel were used to generate the wireless data rates of the 5 air interfaces. To illustrate the delay skew disturbance rejection performance the downlink delays were varied as depicted in Fig. 3. The controller filters were selected as in [11], i.e. lead-lag controllers were used for the inner loops, the skew controllers and the sum controller. The inner loop cross over frequencies were 7 Hz, with half that value being used for the outer loop filters. All lag links provided 20 dB of additional low frequency gain.

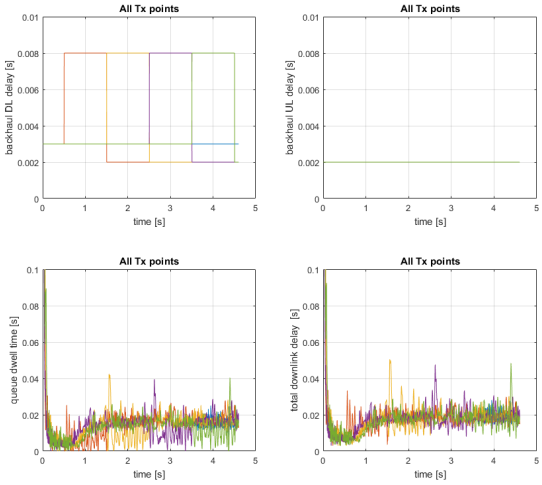

Fig. 3. Downlink and uplink delays, together with the resulting queue dwell times and total downlink delays. Each data path is represented with a separate color.

All controller filters were then discretized using Tustin's approximation as described in [20]

$$s \to \frac{2}{T_s} \frac{1 - q^{-1}}{1 + q^{-1}}. \tag{24}$$

The sampling period was $T_s = 3.0$ ms and q^{-1} denotes the time shift operator.

The delay skew control results appear in Fig. 4, where it can be seen that delay variations are regulated away, exactly as intended. As can be seen in Fig. 3, the delay skew controller varies the dwell times of data packets in the buffers of the transmission nodes to achieve the control objective. It can also be observed that when the downlink fronthaul delay of a data path increases, the corresponding skew control channel becomes less well damped. However, the other skew control channels and sum control channel are not affected. This is believed to be an effect of the decoupling and the symmetric design of the control channels, as recommended by Theorems 1 and 2.

V. Conclusion

A MIMO delay skew control algorithm for packet data flow control in 5G wireless systems was presented. The controller is expected to provide key functionally for example for ultra-reliable machine type communications when multi-connectivity is deployed for high 5G carrier frequencies. The paper analyzed the reference signal tracking and disturbance rejection properties of the closed loop system. The conclusions indicate advantages when the multi-connectivity transmission is symmetric between the different data paths. The disturbance rejection properties benefit by well designed inner loops, thereby obeying the cascade control principle. Both these results are practically important since they provide guidelines for the design of wireless 5G delay critical multi-point transmission networks.

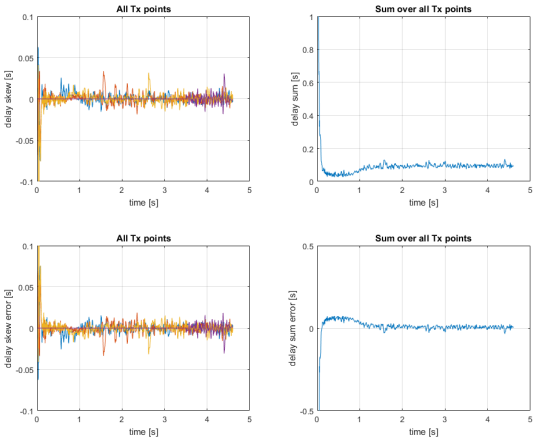

Fig. 4. Delay skews, delay sum and the corresponding errors. Each data path is represented with a separate color.

VI. Acknowledgements

This research was supported under Australian Research Council's Linkage Projects funding scheme (project number LP150100757).

References

[1] R. H. Middleton, T. Wigren, K. Lau, and R. Delgado. Data flow delay equalization for feedback control applications using 5G wireless dual connectivity. *Proc. IEEE VTC 2017 Spring,* Sydney, Australia, June 4-7, 2017.

[2] Ericsson AB. 5G Radio Access - Research and Vision. *Ericsson White Paper 284 23-3204 Uen*, June, 2013. Available: http://www.ericsson.com/res/docs/whitepapers/wp-5g.pdf.

[3] T. S. Rappaport. The renaissance of wireless communications in the massively broadband era. *Plenary talk, IEEE VTC-2012 Fall*, Quebec City, Quebec, Cananda, Sep. 3-6, 2012.

[4] T. S. Rappaport, R. W. Heath Jr., R. C. Daniels, and J. N Murdock. *Millimeter Wave Wireless Communications*. Prentice Hall, Westford, MA, 2014.

[5] T. Wigren, D Colombi, B. Thors, and J.-E. Berg. Implication of RF EMF exposure limitation on 5G data rates above 6 GHz. In *Proc. IEEE VTC 2015 Fall, Boston, MA*, 2015. DOI: 10.1109/VTC-Fall.2015.7390974.

[6] J. Baillieul. Feedback designs for controlling device arrays with communication channel bandwidth constraints. In *Proc. ARO Workshop Smart Structures, Pennsylvania State Univ., Aug. 16-18*, 1999.

[7] R. W. Brocket and D. Liberzon. Quantized feedback stabilization of linear systems. *IEEE Trans. Automat. Contr.*, 45(7):1279–1289, 2000.

[8] G. N. Nair and R. J. Evans. Stabilization with data-rate-limited feedback: tightest attainable bound. *Syst. Contr. Lett.*, 41(1):49–56, 2000.

[9] T Samad. Control systems and the internet of things. *IEEE Control Systems*, 36(1):13–16, 2016.

[10] T. Wigren. Robust $\mathcal{L}_2$ stable networked control of wireless packet queues over delayed internet connections. *IEEE Trans. Contr. Syst. Technol.*, 24:502–513, 2016. DOI: 10.1109/TCST.2015.2455933.

[11] T. Wigren, K. Lau, R. Delgado, and R. H. Middleton. Delay skew packet flow control in 5G wireless systems with dual connectivity. *submitted*, 2016.

[12] R. Srikant and L. Ying. *Communication Networks - An Optimization, Control and Stochastic Networks Perspective*. Cambridge University Press, Padstow, Cornwall, UK, 2014.

[13] R. Delgado, T. Wigren, K. Lau, and R. H. Middleton. Stability properties of a MIMO data flow controller. *Technical Report*, Univ. Newcastle, Newcastle, Australia, August, 2017. Available: http://hdl.handle.net/1959.13/1344681.

[14] R. Delgado, R. H. Middleton, K. Lau, and T. Wigren. Stability properties of a MIMO data flow controller. *submitted*, 2017.

[15] R. Delgado, K. Lau, R. H. Middleton, and T. Wigren. Networked delay control for 5G wireless machine type communications using multi-connectivity. *submitted*, 2016.

[16] T. Wigren and R. Karaki. Globally stable wireless data flow control. *To appear in IEEE Trans. Contr. Network Systems*, 2017. DOI: 10.1109/TCNS.2016.2619906.

[17] A. Megretski and A. Rantzer. System analysis via integral quadratic constraints. *IEEE Trans. on Automatic Control*, 42(6):819–830, 1997.

[18] T. Wigren. Low frequency sensitivity function constraints for nonlinear $\mathcal{L}_2$-stable networked control. *Asian J. Contr.*, 18:1200–1218, 2016. DOI: 10.1002/asjc.1241.

[19] T. Glad and L. Ljung. *Control Theory*. Bodmin, UK: Taylor and Francis, 2000.

[20] A. V. Oppenheim and R. W. Schafer. *Digital Signal Processing*. Prentice Hall, Englewood Cliffs, NJ, 1975.